

AlGaAs/GeSn p-i-n diode interfaced with ultrathin Al₂O₃

Yang Liu, Yiran Li, Sudip Acharya, Jie Zhou, *Member, IEEE*, Jiarui Gong, *Member, IEEE*, Alireza Abrand, Yi Lu, Daniel Vincent, Samuel Haessly, Parsian K. Mohseni, Shui-Qing Yu, *Senior Member, IEEE*, and Zhenqiang Ma, *Fellow, IEEE*

Abstract— This study presents the fabrication and characterizations of an Al_{0.3}Ga_{0.7}As/Ge_{0.87}Sn_{0.13}/GeSn p-i-n double heterostructure (DHS) diode following the grafting approach for enhanced optoelectronic applications. By integrating ultra-thin Al₂O₃ as a quantum tunneling layer and enhancing interfacial double-side passivation, we achieved a heterostructure with a substantial 1.186 eV conduction band barrier between AlGaAs and GeSn, along with a low interfacial density of states. The diode demonstrated impressive electrical characteristics with high uniformity, including a mean ideality factor of 1.47 and a mean rectification ratio of 2.95×10^3 at ± 2 V across 326 devices, indicating high-quality device fabrication. Comprehensive electrical characterizations, including C-V and I-V profiling, affirm the diode's capability to provide robust electrical confinement and efficient carrier injection. These properties make the Al_{0.3}Ga_{0.7}As/Ge_{0.87}Sn_{0.13}/GeSn DHS a promising candidate for next-generation electrically pumped GeSn lasers, potentially operable at higher temperatures. Our results provide a viable pathway for further advancements in various GeSn-based devices.

Index Terms— Aluminum gallium arsenide, germanium tin, double heterostructure, grafting, electrical confinement, interface, ultrathin oxide

I. INTRODUCTION

Germanium-tin (GeSn) alloy has emerged as a pivotal material within the group-IV semiconductors, offering substantial potential for monolithic optoelectronic integrated circuits in the recent years [1-3]. Its ability to transition from an indirect to a direct bandgap around 8% tin composition [4], positions GeSn as a viable mid-wave infrared light source compatible with CMOS technology on silicon substrates [5]. Since the achievement of the first optically pumped GeSn laser at 90 K in 2015 [6], advancements have significantly enhanced

the performance of these lasers. GeSn microdisk lasers utilizing tensile strain can now operate at 300 K with an energy density of $550 \text{ kW} \cdot \text{cm}^{-2}$ [7], alongside other strain-managed film-based devices [8-10].

The development of electrically pumped GeSn lasers has garnered attention due to their potential on-chip applications [11]. The inaugural electrically injected Fabry-Perot GeSn laser, demonstrated in 2020, operated in a pulsed mode, delivering an output of 2.7 mW per facet at 10 K, with a maximum lasing temperature of 100 K [12]. Advances in SiGeSn/GeSn/Ge p-i-n double heterostructures (DHS) have pushed the operational temperature limit to 140 K, with a lasing threshold of 0.756 kA/cm^2 at 77 K [13]. SiGeSn is lattice-matched and forms a Type-I band alignment with GeSn active layer, serving as a carrier injection and optical confinement cap [1, 14, 15]. Key challenges to achieving higher operating temperatures and reducing threshold currents have been identified, including metal contact scattering losses, electron confinement in the cap layer, and free carrier absorption [16]. At the cap/active region interface, Si_{0.03}Ge_{0.89}Sn_{0.08} provides a 114 meV conduction band barrier to Ge_{0.89}Sn_{0.11}, facilitating electron confinement, while the GeSn buffer serves as the hole barrier. Such DHS confinement works well at low temperatures, but is ineffective as it approaches room temperature due to the thermally excited carrier leakage [17]. Developing DHS with enhanced electron confinement barriers is critical for improving performance.

Semiconductor grafting, an innovative technology, expands the possibilities for creating heterostructures from dissimilar materials, despite their lattice mismatches and structural differences [18]. This technique utilizes an ultrathin dielectric layer, such as an ultrathin oxide as an interface, which functions both as a double-side passivation and a quantum tunneling layer between two single-crystalline semiconductors [19-26]. This approach facilitates the formation of nearly ideal lattice-mismatched heterojunctions. It has been demonstrated to be effective in applications requiring high power [22, 26], high frequency [27], and advanced optoelectronic capabilities [19, 25], proving its utility and effectiveness.

In this study, we employed the grafting approach to demonstrate a high-quality GeSn-based double heterostructure, enhancing electron confinement and substantially improving the rectification of the GeSn/Ge-based diodes. The Al_{0.3}Ga_{0.7}As/Ge_{0.87}Sn_{0.13}/GeSn p-i-n double heterostructure was successfully fabricated using this grafting method. The diode exhibited remarkable performance metrics, including a 1.186 eV conduction band barrier, a mean ideality factor of 1.47, and

Yang Liu and Yiran Li contributed equally to this letter.

Yang Liu, Yiran Li, Jie Zhou, Jiarui Gong, Yi Lu, Daniel Vincent, Samuel Haessly, and Zhenqiang Ma are with the Department of Electrical and Computer Engineering, University of Wisconsin-Madison, Madison, WI 53706, USA. (e-mail: mazq@engr.wisc.edu).

Alireza Abrand and Parsian K. Mohseni are with the Microsystems Engineering, Rochester Institute of Technology, Rochester, NY, 14623. (e-mail: pkmeen@rit.edu)

Sudip Acharya and Shui-Qing Yu are with Department of Electrical Engineering, University of Arkansas, Fayetteville, AR 72701 USA. (e-mail: syu@uark.edu).

This work is supported by Air Force Office of Scientific Research under grant FA9550-19-1-0102 and National Science Foundation under Award No. 2235443.

a mean on/off ratio of 2.95×10^3 across 326 devices, featuring a uniformly low density of interface traps (D_{it}). Compared to other GeSn heterojunctions developed through CVD epitaxial growth and nanomembrane transfer, our device demonstrated the highest on-off ratio and electron confinement. These comprehensive evaluations affirm the effectiveness of our approach in GeSn-based devices, paving the way for its potential use in electrically pumped GeSn lasers in the near future.

II. EXPERIMENT

The fabrication process flow of the Al_{0.3}Ga_{0.7}As/Ge_{0.87}Sn_{0.13}/GeSn DHS is illustrated in **Fig. 1**. An epitaxially grown AlGaAs stack, consisting of a 100 nm 1×10^{19} cm⁻³ p⁺-GaAs on top of the 500 nm 1×10^{18} cm⁻³ p-AlGaAs active layer and an Al_{0.95}Ga_{0.05}As scarified layer, was lifted off from its hosting substrate using a polydimethylsiloxane (PDMS) stamp after treatment with 49% hydrofluoric acid (HF), as shown in **Fig. 1(a)(b)**. Meanwhile, the cleaned and polished GeSn epi substrate, containing a 310nm i-Ge_{0.87}Sn_{0.13} layer (post-polishing) and a 600nm GeSn grading buffer layer (8%-13% Sn), was loaded into atomic layer deposition (ALD) system, following a deposition of 5 cycles Al₂O₃ (0.11 nm/cycle) on the surface at 200 °C (**Fig. 1(c)(d)**). The released AlGaAs layer was transfer-printed onto the ALD-coated GeSn substrate via the PDMS stamp (**Fig. 1(e)**), followed by rapid thermal annealing (RTA) at 200 °C for 30 min under N₂ ambient to form chemical bonding (**Fig. 1(f)**). Mesa etching was performed using an inductively coupled plasma (ICP) etcher to open windows on the heterostructure for n-ohmic contacts. Subsequently, n-ohmic contact metal (Ni/Au/Cu/Au: 10/10/100/10 nm) was deposited on the ICP-exposed n⁺-GeSn buffer layer and p-ohmic contact metal (Ti/Pt/Au/Cu/Au: 15/50/10/100/50 nm) was deposited on the p⁺-GaAs layer using electron beam metal evaporator (**Fig. 1(g)**). A device isolation dry etching process was then carried out by etching away the surrounding AlGaAs and GeSn following isolation patterning

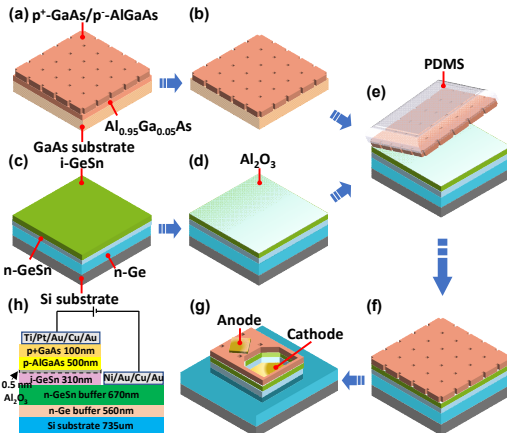


Fig. 1 Fabrication process flow of the AlGaAs/GeSn/GeSn DHS. (a) p⁺-GaAs/p-AlGaAs stack sample structure after hole etching; (b) Al_{0.95}Ga_{0.05}As scarified layer selectively removed by HF to release the p-AlGaAs layer; (c) GeSn epi structure; (d) 0.5 nm Al₂O₃ deposited on the surface using ALD; (e) Released AlGaAs layer picked up by a PDMS stamp and transfer-printed to the GeSn substrate; (f) Heterostructure formed after RTA; (g) Diode fabricated following conventional photolithography, dry etching, and ohmic contact metal deposition; (h) Schematic illustration of the AlGaAs/GeSn/GeSn DHS.

lithography. Finally, all diodes were passivated with 80 cycles of Al₂O₃ (~ 8 nm) using ALD. The schematic structure of the AlGaAs/GeSn/GeSn DHS is shown in **Fig. 1(h)**.

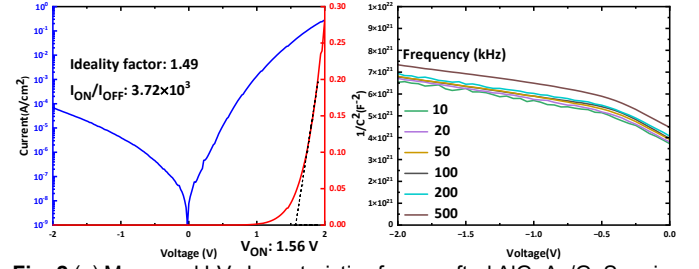


Fig. 2 (a) Measured I-V characteristics from grafted AlGaAs/GeSn p-i-n DHS in the range of ± 2 V (inset: optical image of 4 devices); (b) Measured $1/C^2$ of the diode as a function of bias voltage at multiple frequencies from 20 to 500 kHz.

III. RESULTS AND DISCUSSION

AlGaAs provides a higher conduction band energy offset than Ge and SiGeSn, along with a lower refractive index compared to GeSn. The detailed band diagram, showing a 1.186 eV conduction band offset as determined by the X-ray photoelectron spectroscopy, can be found in our recent work []. The current-voltage (I-V) characteristics of the AlGaAs/GeSn/GeSn DHS diode at 300K were measured using a Keithley 4200 Semiconductor Parameter Analyzer, with results presented on both linear and semi-logarithmic scales in **Fig. 2(a)**. The inset of **Fig. 2(a)** shows an optical image of 4 devices. To avoid the influence of photocurrent, all measurements were conducted under dark conditions. The diode exhibited significant rectification, with a ratio of 3.72×10^3 at ± 2 V. At a reverse bias of -2 V, the current density was notably low at 6.9×10^{-5} A/cm², indicative of low surface defects and high-quality device fabrication. The I-V characteristics were analyzed using the I-V equation to derive series resistance (R_s) [28]. We determined an ideality factor (n) of 1.49, a good value largely attributable to the interfacial passivation by Al₂O₃, which effectively reduces D_{it} . This low ideality factor confirms excellent carrier injection efficiency within the diode [29, 30]. The series resistance (R_s) obtained through analysis was 1.2 k Ω ·cm², possibly influenced by the annealing temperature limits of the ohmic contact metal and potential tin segregation at elevated temperatures [31]. Additionally, the turn-on voltage of the diode was derived by fitting the I-V curve in the linear region from 1.5 V to 2 V at a current of approximately 0.15 A, extrapolating to zero to yield a value of 1.56 V. At a forward bias of +2 V, the current density and ON resistance were measured as 0.28 A/cm² and 7.09 Ω ·cm².

Furthermore, to understand the D_{it} value between AlGaAs and GeSn, the capacitance-voltage (C-V) characteristics of the Al_{0.3}Ga_{0.7}As/Ge_{0.87}Sn_{0.13}/GeSn DHS diodes were measured by the Keithley 4200. Notably, as shown in the **Fig. 2(b)**, a negligible frequency dispersion was observed in the C-V curves across a frequency range from 20 kHz to 200 kHz, affirming the device stability [26]. The non-linear behavior of the $1/C^2 - V$ plot near 0V indicates the presence of defects in the GeSn layer, likely due to challenges encountered during the growth process [32]. A slight discrepancy observed at 500 kHz likely results from interface defects becoming excited at higher frequencies. Overall, the minimal dispersion in the plot

signifies excellent interface quality of the AlGaAs/GeSn and indicates an acceptable D_{it} .

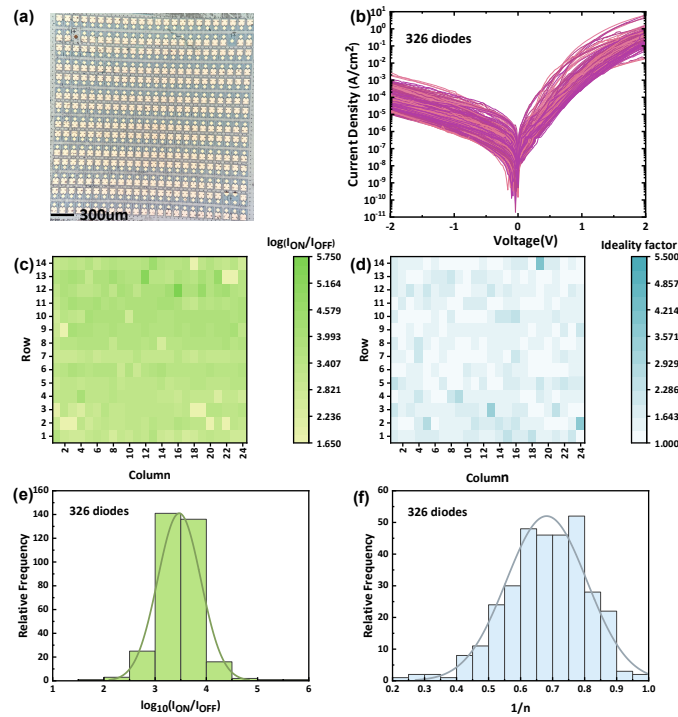


Fig. 3 (a) Optical micrograph of the fabricated diode array; (b) I-V characteristics across 326 devices; (c)(d) Mapping of the 326 devices' rectification ratio and ideality factor; (e)(f) Distribution of the 326 devices' rectification ratio and the reciprocal of ideality factor.

A statistical analysis of the current-voltage characteristics of 326 devices across the entire sample is depicted in **Fig. 3(b)**, measured from the sample shown in **Fig. 3(a)**. The mapping and distribution of the rectification ratios at ± 2 V and ideality factors for these 326 diodes are plotted in **Fig. 3(c)(e)** and **Fig. 3(d)(f)**, respectively. Both the base-10 logarithmic rectification ratio ($\text{Log}_{10}(I_{ON}/I_{OFF})$) and the reciprocal of the ideality factor ($1/n$) followed Gaussian distributions, with mean values and standard deviations of 3.47 ± 0.42 and 0.68 ± 0.13 , respectively. Consequently, the mean diode rectification ratio is calculated to be 2.95×10^3 at ± 2 V. Using the rule of uncertainty propagation, the mean ideality factor (n) is determined to be 1.47 ± 0.28 . The consistency in the diode rectification ratio and ideality factor indicates a uniform interfacial condition, affirming the feasibility of our DHS structure approach for future AlGaAs/GeSn electrically pumped laser device applications. **Fig. 4** benchmarks the conduction band offset and

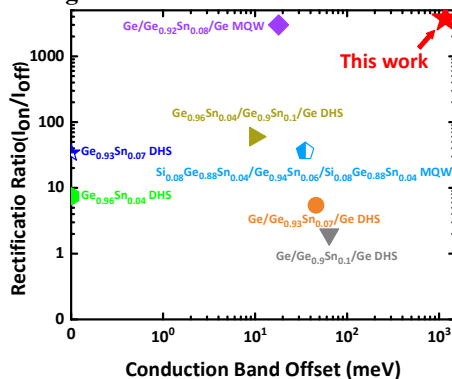


Fig. 4 Benchmarks of the conduction band offset and rectification ratio for similar GeSn based p-i-n double heterostructures.

rectification ratio against those from previous studies on similar GeSn p-i-n double heterostructures developed through epitaxy and transfer printing. Our work exhibits a large conduction band offset with the highest on/off ratio[30, 31, 33-37].

IV. CONCLUSION

In this study, we fabricated and characterized an AlGaAs/GeSn/GeSn double heterostructure diode using the grafting approach. The resulting structure exhibited a 1.186 eV conduction band barrier between AlGaAs and GeSn, a low interfacial density of states, and robust electrical characteristics. This heterostructure ensures adequate electrical confinement, making it a promising approach for fabricating electrically pumped GeSn lasers possibly operating at higher temperatures.

REFERENCES

- [1] S. Wirths, D. Buca, and S. Mantl, "Si-Ge-Sn alloys: From growth to applications," *Prog. Cryst. Growth Charact. Mater.*, Review vol. 62, no. 1, pp. 1-39, Mar 2016, doi: 10.1016/j.pcrysgrow.2015.11.001.
- [2] S. Zaima, O. Nakatsuka, N. Taoka, M. Kurosawa, W. Takeuchi, and M. Sakashita, "Growth and applications of GeSn-related group-IV semiconductor materials," *Sci. Technol. Adv. Mater.*, Review vol. 16, no. 4, p. 22, Aug 2015, Art no. 043502, doi: 10.1088/1468-6996/16/4/043502.
- [3] J. Zheng, Z. Liu, C. L. Xue, C. B. Li, Y. H. Zuo, B. W. Cheng, and Q. M. Wang, "Recent progress in GeSn growth and GeSn-based photonic devices," *J. Semicond.*, Review vol. 39, no. 6, p. 6, Jun 2018, Art no. 061006, doi: 10.1088/1674-4926/39/6/061006.
- [4] G. E. Chang, S. W. Chang, and S. L. Chuang, "Strain-Balanced Ge₂Sn_{1-x}Si_xGe_ySn_{1-x-y} Multiple-Quantum-Well Lasers," *IEEE J. Quantum Electron.*, Article vol. 46, no. 12, pp. 1813-1820, Dec 2010, doi: 10.1109/jqe.2010.2059000.
- [5] V. Reboud, A. Gassenq, J. M. Hartmann, J. Widiez, L. Virost, J. Aubin, K. Guillois, S. Tardif, J. M. Fédéli, N. Pauc, A. Chelnokov, and V. Calvo, "Germanium based photonic components toward a full silicon/germanium photonic platform," *Prog. Cryst. Growth Charact. Mater.*, Review vol. 63, no. 2, pp. 1-24, Jun 2017, doi: 10.1016/j.pcrysgrow.2017.04.004.
- [6] S. Wirths, R. Geiger, N. von den Driesch, G. Mussler, T. Stoica, S. Mantl, Z. Ikonik, M. Luysberg, S. Chiussi, J. M. Hartmann, H. Sigg, J. Faist, D. Buca, and D. Grützmacher, "Lasing in direct-bandgap GeSn alloy grown on Si," *Nat. Photonics*, Article vol. 9, no. 2, pp. 88-92, Feb 2015, doi: 10.1038/nphoton.2014.321.
- [7] D. Buca, A. Bjelajac, D. Spirito, O. Concepción, M. Gromovyi, E. Sakat, X. Lafosse, L. Ferlazzo, N. von den Driesch, Z. Ikonik, D. Grützmacher, G. Capellini, and M. El Kurdi, "Room Temperature Lasing in GeSn Microdisks Enabled by Strain Engineering," *Adv. Opt. Mater.*, Article vol. 10, no. 22, p. 9, Nov 2022, Art no. 2201024, doi: 10.1002/adom.202201024.
- [8] D. Rainko, Z. Ikonik, A. Elbaz, N. von den Driesch, D. Stange, E. Herth, P. Boucaud, M. El Kurdi, D. Grützmacher, and D. Buca, "Impact of tensile strain on low Sn content GeSn lasing," *Sci Rep*, Article vol. 9, p. 9, Jan 2019, Art no. 259, doi: 10.1038/s41598-018-36837-8.
- [9] A. Elbaz, D. Buca, N. von den Driesch, K. Pantzas, G. Patriarche, N. Zerounian, E. Herth, X. Checoury, S. Sauvage, I. Sagnes, A. Foti, R. Ossikovski, J. M. Hartmann, F. Boeuf, Z. Ikonik, P. Boucaud, D. Grützmacher, and M. El Kurdi, "Ultra-low-threshold continuous-wave and pulsed lasing in tensile-strained GeSn alloys," *Nat. Photonics*, Article vol. 14, no. 6, pp. 375-+, Jun 2020, doi: 10.1038/s41566-020-0601-5.
- [10] J. Chrétien, N. Pauc, F. A. Pilon, M. Bertrand, Q. M. Thai, L. Casiez, N. Bernier, H. Dansas, P. Gergaud, E. Delamadeleine, R. Khazaka, H. Sigg, J. Faist, A. Chelnokov, V. Reboud, J. M. Hartmann, and V. Calvo, "GeSn Lasers Covering a Wide Wavelength Range Thanks to Uniaxial Tensile Strain," *ACS Photonics*, Article vol. 6, no. 10, pp. 2462-2469, Oct 2019, doi: 10.1021/acsp Photonics.9b00712.
- [11] B. Dutt, H. Lin, D. S. Sukhdeo, B. M. Vulovic, S. Gupta, D. Nam, K. C. Saraswat, and J. S. Harris, "Theoretical Analysis of GeSn Alloys as a Gain Medium for a Si-Compatible Laser," *IEEE J. Sel. Top. Quantum Electron.*, Article vol. 19, no. 5, p. 6, Sep-Oct 2013, Art no. 1502706, doi: 10.1109/jstqe.2013.2241397.
- [12] Y. Y. Zhou, Y. H. Miao, S. Ojo, H. Tran, G. Abernathy, J. M. Grant, S. Amoah, G. Salamo, W. Du, J. F. Liu, J. Margetis, J. Tolle, Y. H. Zhang, G. Sun, R. A. Soref, B. H. Li, and S. Q. Yu, "Electrically injected GeSn lasers on Si operating up to 100 K," *Optica*, Article vol. 7, no. 8, pp. 924-928, Aug 2020, doi: 10.1364/optica.395687.
- [13] S. Acharya, H. Stanchu, R. Kumar, S. Ojo, M. Alher, M. Benamara, G.-E. Chang, B. Li, W. Du, and S.-Q. Yu, "Electrically Injected mid-infrared GeSn laser on Si operating at 140 K," *IEEE J. Sel. Top. Quantum Electron.*, pp. 1-8, 2024, doi: 10.1109/jstqe.2024.3430060.
- [14] G. Sun, R. A. Soref, and H. H. Cheng, "Design of a Si-based lattice-matched room-temperature GeSn/GeSiSn multi-quantum-well mid-infrared laser diode," *Optics Express*, Article vol. 18, no. 19, pp. 19957-19965, Sep 2010, doi: 10.1364/oe.18.019957.
- [15] D. Stange, N. von den Driesch, T. Zabel, F. Armand-Pilon, D. Rainko, B. Marzban, P. Zaumseil, J. M. Hartmann, Z. Ikonik, G. Capellini, S. Mantl, H. Sigg, J. Witzens, D. Grützmacher, and D. Buca, "GeSn/SiGeSn Heterostructure and Multi Quantum Well Lasers," *ACS Photonics*, Article vol. 5, no. 11, pp. 4628-4636, Nov 2018, doi: 10.1021/acsp Photonics.8b01116.
- [16] Y. Y. Zhou, S. Ojo, C. W. Wu, Y. H. Miao, H. Tran, J. M. Grant, G. Abernathy, S. Amoah, J. Bass, G. Salamo, W. Du, G. E. Chang, J. F. Liu, J. Margetis, J. Tolle, Y. H. Zhang, G. Sun, R. A. Soref, B. H. Li, and S. Q. Yu, "Electrically injected GeSn lasers with peak wavelength up to 2.7 μm," *Photonics Res.*, Article vol. 10, no. 1, pp. 222-229, Jan 2022, doi: 10.1364/prj.443144.
- [17] A. R. Ellis, D. A. Duffy, I. P. Marko, S. Acharya, W. Du, S. Q. Yu, and S. J. Sweeney, "Challenges for room temperature operation of electrically pumped GeSn lasers," *Sci Rep*, Article vol. 14, no. 1, p. 11, May 2024, Art no. 10318, doi: 10.1038/s41598-024-60686-3.
- [18] D. Liu, S. J. Cho, J.-H. Seo, K. Kim, M. Kim, J. Shi, X. Yin, W. Choi, C. Zhang, and J. Kim, "Lattice-mismatched semiconductor heterostructures," *arXiv preprint arXiv:1812.10225*, 2018.
- [19] J. Zhou, H. Wang, P. R. Huang, S. Xu, Y. Liu, J. Gong, J. Shen, D. Vicent, S. Haessly, and A. Abrand, "GaAs/GeSn/Ge n-i-p diodes and light emitting diodes formed via grafting," *J. Vac. Sci. Technol. B*, vol. 42, no. 4, 2024.
- [20] J. Zhou, J. Gong, S. Lal, J. Kim, W. Lin, C. Chen, C. Li, Y. Lu, S. Qiu, and Y. Dong, "Characteristics of native oxides-interfaced GaAs/Ge np diodes," *IEEE Electron Device Lett.*, 2024.
- [21] J. Zhou, J. R. Gong, M. Sheikhi, A. Dheenani, Q. X. Wang, H. Abbasi, Y. Liu, C. Adamo, P. Marshall, N. Wriedt, C. Cheung, Y. R. Li, S. Y. Qiu, X. H. Li, T. K. Ng, Q. Q. Gan, V. Gambin, B. S. Ooi, S. Rajan, and Z. Q. Ma, "Synthesis and characteristics of a monocrySTALLINE GaAs/Beta-Ga₂O₃ p-n heterojunction," *Applied Surface Science*, Article vol. 663, p. 8, Aug 2024, Art no. 160176, doi: 10.1016/j.apsusc.2024.160176.
- [22] S. W. Xie, M. T. Alam, J. R. Gong, Q. C. Lin, M. Sheikhi, J. Zhou, F. Alema, A. Osinsky, S. S. Pasayat, Z. Q. Ma, and C. Gupta, "0.86 kV p-Si/(001)-Ga₂O₃ Heterojunction Diode," *IEEE Electron Device Lett.*, vol. 45, no. 3, pp. 444-447, Mar 2024, doi: 10.1109/led.2024.3352515.
- [23] J. R. Gong, J. Zhou, A. Dheenani, M. Sheikhi, F. Alema, T. K. Ng, S. S. Pasayat, Q. Q. Gan, A. Osinsky, V. Gambin, C. Gupta, S. Rajan, B. S. Ooi, and Z. Q. Ma, "Band alignment of grafted monocrySTALLINE Si (001)/Beta-Ga₂O₃ (010) p-n heterojunction determined by X-ray photoelectron spectroscopy," *Applied Surface Science*, Article vol. 655, p. 6, May 2024, Art no. 159615, doi: 10.1016/j.apsusc.2024.159615.
- [24] J. R. Gong, D. Kim, H. Jang, F. Alema, Q. X. Wang, J. Zhou, Y. R. Li, T. K. Ng, S. Y. Qiu, Y. Liu, M. Sheikhi, Y. Lu, R. Singh, X. Su, H. N. Abbasi, Q. C. Lin, S. W. Xie, K. Chabak, G. Jessen, C. Cheung, V. Gambin, S. S. Pasayat, A. Osinsky, B. S. Ooi, C. Gupta, and Z. Q. Ma, "Characteristics of grafted monocrySTALLINE Si/β-Ga₂O₃ p-n heterojunction," *Appl. Phys. Lett.*, Article vol. 124, no. 26, p. 7, Jun 2024, Art no. 262101, doi: 10.1063/5.0208744.
- [25] D. Liu, S. J. Cho, J. Park, J. R. Gong, J. H. Seo, R. Dalmau, D. Y. Zhao, K. Kim, M. Kim, A. R. K. Kalapala, J. D. Albrecht, W. D. Zhou, B. Moody, and Z. Q. Ma, "226 nm AlGaIn/AlN UV LEDs using p-type Si for hole injection and UV reflection," *Appl. Phys. Lett.*, Article vol. 113, no. 1, p. 5, Jul 2018, Art no. 011111, doi: 10.1063/1.5038044.
- [26] S. W. Xie, M. Sheikhi, S. N. Xu, M. T. Alam, J. Zhou, L. Mawst, Z. Q. Ma, and C. Gupta, "p-GaAs/n-Ga₂O₃ heterojunction diode with breakdown voltage of ~800 V," *Appl. Phys. Lett.*, Article vol. 124, no. 7, p. 6, Feb 2024, Art no. 073503, doi: 10.1063/5.0181056.
- [27] K. Kim, T. J. Kim, H. L. Zhang, D. Liu, Y. H. Jung, J. R. Gong, and Z. Q. Ma, "AlGaIn/GaN Schottky-Gate HEMTs With UV/O₃-Treated Gate Interface," *IEEE Electron Device Lett.*, Article vol. 41, no. 10, pp. 1488-1491, Oct 2020, doi: 10.1109/led.2020.3019339.
- [28] S. Kim, J. Gupta, N. Bhargava, M. Coppinger, and J. Kolodzey, "Current-Voltage Characteristics of GeSn/Ge Heterojunction Diodes Grown by Molecular Beam Epitaxy," *IEEE Electron Device Lett.*, Article vol. 34, no. 10, pp. 1217-1219, Oct 2013, doi: 10.1109/led.2013.2278371.

- [29] R. Bansal, Y. T. Jheng, K. C. Lee, H. H. Cheng, and G. E. Chang, "GeSn Vertical Heterostructure p-i-n Waveguide Light Emitting Diode for 2 μm Band Silicon Photonics," *IEEE Electron Device Lett.*, Article vol. 44, no. 3, pp. 364-367, Mar 2023, doi: 10.1109/led.2023.3236847.
- [30] Q. M. Chen, Y. D. Jung, H. Zhou, S. T. Wu, X. Gong, Y. C. Huang, K. H. Lee, L. Zhang, D. Nam, J. Liu, J. W. Luo, W. J. Fan, and C. S. Tan, "GeSn/Ge Multiquantum-Well Vertical-Cavity Surface-Emitting p-i-n Structures and Diode Emitters on a 200 nm Ge-on-Insulator Platform," *ACS Photonics*, Article vol. 10, no. 6, pp. 1716-1725, May 2023, doi: 10.1021/acsp Photonics.2c01934.
- [31] C. Y. Chang, P. L. Yeh, Y. T. Jheng, L. Y. Hsu, K. C. Lee, H. Li, H. H. Cheng, and G. E. Chang, "Mid-infrared resonant light emission from GeSn resonant-cavity surface-emitting LEDs with a lateral p-i-n structure," *Photonics Res.*, Article vol. 10, no. 10, pp. 2278-2286, Oct 2022, doi: 10.1364/prj.457193.
- [32] N. Taoka, M. Fukudome, W. Takeuchi, T. Arahira, M. Sakashita, O. Nakatsuka, and S. Zaima, "Interaction of Sn atoms with defects introduced by ion implantation in Ge substrate," *J. Appl. Phys.*, Article; Proceedings Paper vol. 115, no. 17, p. 7, May 2014, Art no. 173102, doi: 10.1063/1.4874800.
- [33] T. Pham, W. Du, H. Tran, J. Margetis, J. Tolle, G. Sun, R. A. Soref, H. A. Naseem, B. H. Li, and S. Q. Yu, "Systematic study of Si-based GeSn photodiodes with 2.6 μm detector cutoff for short-wave infrared detection," *Optics Express*, Article vol. 24, no. 5, pp. 4519-4531, Mar 2016, doi: 10.1364/oe.24.004519.
- [34] M. R. M. Atalla, S. Assali, S. Koelling, A. Attiaoui, and O. Moutanabbir, "Dark current in monolithic extended-SWIR GeSn PIN photodetectors," *Appl. Phys. Lett.*, Article vol. 122, no. 3, p. 6, Jan 2023, Art no. 031103, doi: 10.1063/5.0124720.
- [35] Y. Chuang, C. Y. Liu, G. L. Luo, and J. Y. Li, "Electron Mobility Enhancement in GeSn n-Channel MOSFETs by Tensile Strain," *IEEE Electron Device Lett.*, Article vol. 42, no. 1, pp. 10-13, Jan 2021, doi: 10.1109/led.2020.3041051.
- [36] J. Zheng, S. Y. Wang, H. Cong, C. S. Fenrich, Z. Liu, C. L. Xue, C. B. Li, Y. H. Zuo, B. W. Cheng, J. S. Harris, and Q. M. Wang, "Characterization of a Ge_{1-x-y}Si_ySn_x/Ge_{1-x}Sn_x multiple quantum well structure grown by sputtering epitaxy," *Opt. Lett.*, Article vol. 42, no. 8, pp. 1608-1611, Apr 2017, doi: 10.1364/ol.42.001608.
- [37] J. Y. Yang, H. Y. Hu, Y. H. Miao, L. P. Dong, B. Wang, W. Wang, H. Su, R. X. Xuan, and H. M. Zhang, "High-quality GeSn Layer with Sn Composition up to 7% Grown by Low-Temperature Magnetron Sputtering for Optoelectronic Application," *Materials*, Article vol. 12, no. 17, p. 11, Sep 2019, Art no. 2662, doi: 10.3390/ma12172662.